

## Microwave-Assisted Preparation of Zinc-Doped $\beta$ -Tricalcium Phosphate for Orthopedic Applications

Ali Taha Saleh<sup>1\*</sup> and Dheyaa Alameri<sup>2</sup>

<sup>1</sup>Department of Chemistry, College of Science, University of Misan, Misan, Iraq

<sup>2</sup>Department of Physics, College of Science, University of Misan, Misan, Iraq

\* **Corresponding author:**

email: ali\_6222@yahoo.com.sg

Received: May 8, 2020

Accepted: May 30, 2020

DOI: 10.22146/ijc.55931

**Abstract:** A novel two-step methodology delivering zinc into the structure of  $\beta$ -tricalcium phosphate ( $\beta$ -TCP) has been investigated. Incorporating wet precipitation of calcium-deficient apatite [ $\text{Ca}_{9-x}\text{Zn}_x(\text{HPO}_4)(\text{PO}_4)_5(\text{OH})$ ] ( $x = 0.00$ – $1.00$  mol) using a microwave-assisted process followed by two-hour calcination at  $1000$  °C has been conducted to generate a ratio of 1.48 of Zn doped  $\beta$ -TCP. The products were characterized by X-ray diffraction (XRD), Fourier-transform infrared (FTIR) spectrometer, and field emission scanning electron microscope (FESEM). Our results confirmed that the product was crystalline  $\text{Zn}^{2+}$ -doped  $\beta$ -tricalcium phosphate. The incorporation of  $\text{Zn}^{2+}$  into the  $\beta$ -TCP lattice resulted in a shifting of diffraction peaks to higher  $2\theta$  values, which were attributed to the substitution of larger-sized  $\text{Ca}^{2+}$  ions with smaller-sized  $\text{Zn}^{2+}$  ions. A reduction in the intensity of the XRD peaks was also observed due to the reduction in the degree of crystallinity of the samples. Lattice parameters along the  $a$  and  $c$ -axis showed a gradual decrease in length with an increase in the amount of  $\text{Zn}^{2+}$  doping. This decrease was attributed to the replacement of  $\text{Ca}^{2+}$  ion by the smaller-sized  $\text{Zn}^{2+}$  ions. The microstructure of the powders consisted of microscale aggregates fused together. EDX analysis of all samples showed that the  $\text{Zn}^{2+}$  doping had successfully taken place and the amount of  $\text{Zn}^{2+}$  present in the samples was in good agreement with the theoretical values.

**Keywords:** microwave-assisted;  $\beta$ -tricalcium phosphate; zinc; characterization

### ■ INTRODUCTION

Given the wide range of applications for bioceramics, there has been substantial and sustained interest in researching calcium phosphate (CaP)-based ceramics for use in medical applications, such as in orthopedic and dental use, over many years [1-3]. Similar in composition to bones, CaP-based ceramics are generally accepted as bone substitutes and to augment existing bone [4-6]. The medical applications are mainly focused on two CaP ceramics/CaPs, namely tricalcium phosphate/ $\text{Ca}_3(\text{PO}_4)_2$  (TCP), and hydroxyapatite  $\text{Ca}_{10}(\text{PO}_4)_6(\text{OH})_2$  (HA), that possess key properties of resorption and surface induction of bone formation, respectively. Furthermore, ceramics based on HA, with superior osteoconductivity and excellent bone replacement abilities, are proven not to induce immune

responses that lead to toxicity and inflammation in response to their presence in the body [7-8].

CaPs are one of the most common and widely used bioceramic materials used to promote regeneration of bone as a result of its biocompatibility, osteoconductivity, osseointegration, and its similar profile to human bone and teeth [9-10]. There are two crystallographic forms of TCP, that is  $\beta$ -TCP and  $\alpha$ -TCP [11-13]. Heating of the beta form of TCP above  $1100$  °C produces the alpha crystalline phase [14-15].

While both  $\alpha$  and  $\beta$  TCP are chemically similar, their structures and physical properties, such as solubility, are different [16-17]. Consequently, a different performance would be obtained from its use in a biomedical situation, such as for use in dicalcium phosphate (DCP) cements [16,18-19]. Furthermore, the use of  $\alpha$ -TCP is limited as it is resorbed quicker than new

bone [20]. In addition, a DFT assessment has demonstrated that  $\beta$ -TCP has more stability than  $\alpha$ -TCP [17].

Manufacturing conditions for  $\beta$ -TCP offer a variety of methods that are conducted at lower temperatures than required for  $\alpha$ -TCP. For example,  $\beta$ -TCP is formed by the thermal composition of Calcium-Deficient Hydroxy Apatitic CDHAp at temperatures over 800 °C [5]. Furthermore, at a temperature of as low as 50 °C, deposition in the organic medium will produce  $\beta$ -TCP [21-22].  $\beta$ -TCP can also be produced directly from the calcining of the bone.

The excellent properties of  $\beta$ -TCP allow it to be used for many biomedical solutions, including bone cement [22], bioceramics, and dental applications [23]. The bone apatite is non-stoichiometric and comprises of multiple elements (Mg, Mn, Zn, and Na), compounds ( $\text{HPO}_4^{2-}$  and  $\text{CO}_3^{2-}$ ) [5], and metal oxides (MgO and ZnO) [6-7]. These compounds are generally associated with multiple functions of bone apatite, including biological, mechanical, and physiochemical roles [24]. Vital for bone metabolism, zinc (Zn) is a key element that is necessary for bone growth and regeneration, and also osteoclast resorption [8,10-12]. However, the balance of Zn and other elements is vital, as increased levels of zinc and similar elements may induce unwanted consequences [9]. In this study, we describe a novel microwave-based method for doping ions that maintain a 1.48 ratio of Ca/P for producing Zn doped  $\beta$ -TCP. As far as we can ascertain, this is the first report of the insertion of zinc ions and its effect towards the  $\beta$ -TCP lattice. This study represents the first account of the influence of Zn ion substitution on the main parameters of the lattice structure. Specifically, we describe the extent of crystallization and the size of crystals in  $\beta$ -TCP. We propose that  $\beta$ -TCP is an appropriate transporter to moderate the release of zinc for biomedical use.

## ■ EXPERIMENTAL SECTION

### Materials

Reagent grade chemicals and materials were acquired from Qrec (New Zealand), including calcium nitrate ( $\text{Ca}(\text{NO}_3)_2 \cdot 4\text{H}_2\text{O}$ ), diammonium hydrogen

phosphate ( $(\text{NH}_4)_2\text{HPO}_4$ ), ammonium hydroxide ( $\text{NH}_4\text{OH}$ ), and zinc nitrate  $\text{Zn}(\text{NO}_3)_2$ .

### Instrumentation

Physical characteristics, such as phase purity, lattice structure, and extent of crystallinity, were determined by X-ray diffractometry (Bruker D8 Advance XRD). The structural morphology and specific element composition were determined by field emission scanning electron microscopy (FESEM) (Zeiss-LEO 1530) in combination with (EDX) (Oxford instrument, Swift ED 3000). Lastly, the synthesis of functional phosphate groups was confirmed by the standard KBr pellet method using Fourier-transformed infrared spectrometry (FTIR) (Nicolet iS50).

### Procedure

The phase purity, lattice specification, and level of crystallinity of the prepared samples were determined by analysis of five individual areas to obtain the average composition of elements via X-ray diffractometry. The XRD outcomes for the Zn doped  $\beta$ -TCP samples are shown in Fig. 1. The diffractogram shows the  $2\theta$  range between 20°–80° with 1-sec steps of 0.02° conducted at room temperature. All of the peaks detected from the synthesized  $\beta$ -TCP align with the  $\beta$ -TCP phase (JCPDS 09-0169), indicating that the crystalline phases are composed, in the majority, of  $\beta$ -TCP phases.

Crystallinity, denoted by  $X_c$ , is a measure of the proportion of crystalline  $\beta$ -TCP phase in the test volume of powdered sample, and is calculated as follows:

$$X_c = 1 - V_{300/0210} / I_{0210}$$

where  $I_{0210}$  is the intensity (0 2 1 0) reflection of the  $\beta$ -TCP structure, and  $V_{300/0210}$  is the intensity of the hollow between the (3 0 0) and (0 2 1 0) reflections.

Unit cell software (program UnitCell-method of TJB Holland & SAT Redfern 1995) was used to define the lattice parameters.

As previously described [6], a microwave-assisted wet precipitation method was used to synthesize both  $\beta$ -TCP and Zn doped  $\beta$ -TCP with samples produced in molar ratios of Ca/P and (Ca + Zn)/P of 1.48, as seen in Table 1. In brief, a typical reaction to produce  $\beta$ -TCP

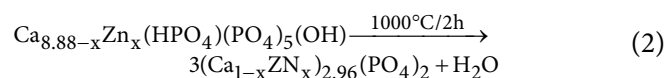
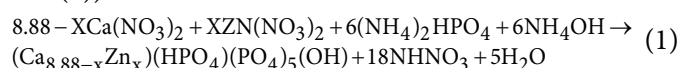
**Table 1.** Molar quantities of reactants used for the synthesis of  $\beta$ -TCP and Zn- $\beta$ -TCP

Sample ID	Ca(NO <sub>3</sub> ) <sub>2</sub> ·4H <sub>2</sub> O (mol)	(NH <sub>4</sub> ) <sub>2</sub> HPO <sub>4</sub> (mol)	Zn(NO <sub>3</sub> ) <sub>2</sub> (mol)	Zn (wt.%)
$\beta$ -TCP	8.88	6	0.00	-
1Zn- $\beta$ -TCP	8.63	6	0.25	2.3
2Zn- $\beta$ -TCP	8.38	6	0.50	6.4
3Zn- $\beta$ -TCP	8.13	6	0.75	7.1
4Zn- $\beta$ -TCP	7.88	6	1.00	8.6

required the dissolution of calcium nitrate (Ca(NO<sub>3</sub>)<sub>2</sub>·4H<sub>2</sub>O) in 100 mL of double-distilled water, to which diammonium hydrogen phosphate (NH<sub>4</sub>)<sub>2</sub>HPO<sub>4</sub>) was dropwise added with stirring. The resulting solution was adjusted to pH 7 with ammonium hydroxide (NH<sub>4</sub>OH), prior to refluxing in a microwave (SHARP, model R-218LS) for 5 min at 800 W. The suspension was filtered before drying for 17 h at a temperature of 80 °C then calcined at 1000 °C for 2 h. Similarly, four concentrations of Zn-doped  $\beta$ -Ca<sub>3</sub>(PO<sub>4</sub>)<sub>2</sub> samples were prepared by the addition of a certain amount of zinc nitrate Zn(NO<sub>3</sub>)<sub>2</sub> into the Ca(NO<sub>3</sub>)<sub>2</sub>·4H<sub>2</sub>O solution. Details of the molar quantities of reactants series are shown in Table 1. In short, this method was the same, with only two exceptions. The successful incorporation of Zn ions required an initial Ca + Zn/P ratio of 1.48 to produce calcium-deficient apatite containing Zn<sup>2+</sup> ion (Ca<sub>8.88-x</sub>Zn<sub>x</sub>)(HPO<sub>4</sub>)(PO<sub>4</sub>)<sub>5</sub>(OH), Zn doped  $\beta$ -TCP (as described in Eq. (1) and (2)), and the pH was adjusted to 7.4 by the dropping (NH<sub>4</sub>OH) solution.

## ■ RESULTS AND DISCUSSION

In this study, the synthesis of  $\beta$ -TCP through a microwave-assisted wet precipitation method involved the preparation of calcium-deficient apatite structure [Ca<sub>8.88</sub>(HPO<sub>4</sub>)(PO<sub>4</sub>)<sub>5</sub>(OH)] by exposing the reaction mixture with a Ca/P molar ratio of 1.48 to 800 W microwave radiations for 5 min. Calcination of this calcium deficient structure at 1000 °C for 2 h furnished the  $\beta$ -TCP. Zn doped  $\beta$ -TCP samples were prepared in the same manner except for the initial Ca + Zn/P ratio that was adjusted to 1.48 to ensure the successful incorporation of the Zn<sup>2+</sup> ions into the structure (Eq. (1) and (2)).



where  $x = [0.00-1.00]$

XRD analysis showed that the inclusion of Zn in the  $\beta$ -TCP lattice shifted the diffraction peaks to higher  $2\theta$  values and simultaneously caused a reduction in the intensity of the XRD peaks. These changes are likely a direct result of ionic radius difference, where the larger Ca<sup>2+</sup> ions (0.99 Å) were replaced by smaller Zn<sup>2+</sup> ions (0.74 Å), as shown in Fig. 1. The largest  $\beta$ -TCP phase peak corresponding to the (0 2 1 0) plane was observed at  $2\theta = 31.392^\circ$ . The diffractions of the (0 2 1 0) plane for samples 1 to 4 of the Zn- $\beta$ -TCP were observed at  $2\theta = 31.441, 31.690, 31.939, \text{ and } 32.188$ , respectively, which is considered to be a consequence of the decreasing levels of crystallinity of these samples [17].

The formation of a solid solution of  $\beta$ -Ca<sub>3</sub>(PO<sub>4</sub>)<sub>2</sub> and Zn<sup>2+</sup> ions can be confirmed since the XRD patterns did not exhibit any additional peaks. Applying the Debye-Scherrer equation generated an estimated crystallite size of 36 nm for  $\beta$ -TCP. As the level of Zn<sup>2+</sup> doping increased, the a and c axes of the lattice structure decreased in length, which is attributed to the replacement of the Ca<sup>2+</sup> ion by the smaller-size Zn<sup>2+</sup> ion, as seen in Table 2 [25]. The decreases in the (4Zn- $\beta$ -TCP) sample were 10.4375 to 10.4276 Å and 37.3645 to 37.2035 Å, for the a and c axes, respectively. The unit cell volume was also reduced from 3526.3572 to 3512.6672 Å as a consequence of the smaller size of Zn<sup>2+</sup> in the structure [6,20] (Table 2).

The FTIR spectra, recorded at a wavenumber range of 400–4000 cm<sup>-1</sup> in transmission mode with 32 scans and 4 cm<sup>-1</sup> resolutions, of Zn<sup>2+</sup> doped  $\beta$ -TCP calcined at 1000 °C is shown in Fig. 2. The bands observed at 548 and 610 cm<sup>-1</sup> correspond to the bending mode ( $\nu_4$ ) of the

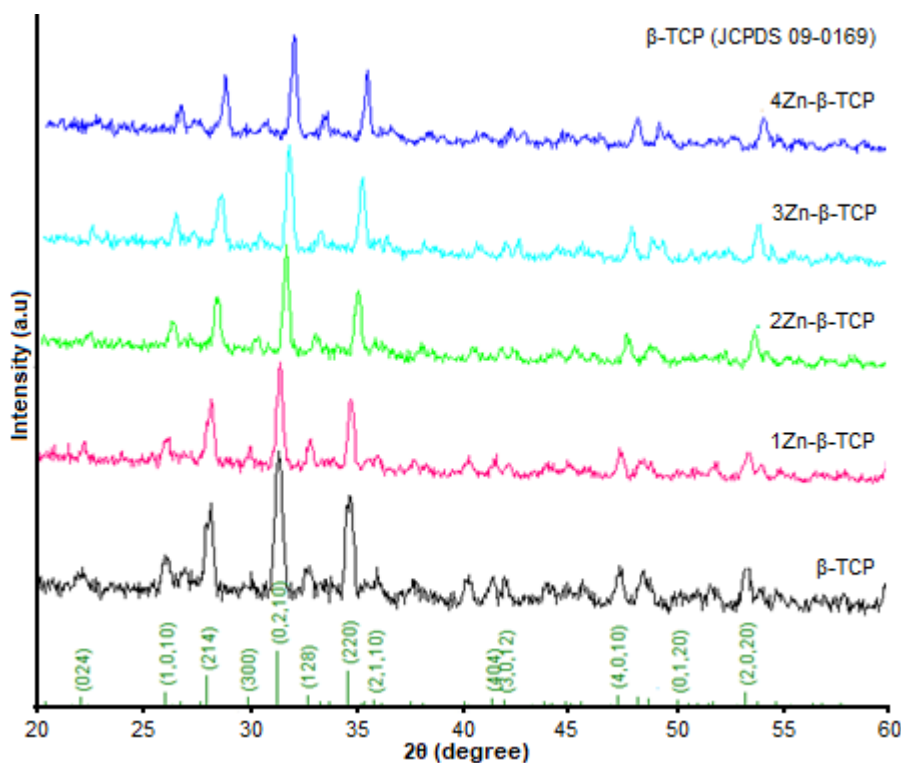


Fig 1. XRD pattern of a  $\beta$ -TCP and Zn- $\beta$ -TCP

Table 2. Lattice parameters of  $\beta$ -TCP substituted with different amounts of  $\text{Zn}^{2+}$  ions and the degree of crystallinity

Samples	Chemical formula	Lattice parameter			Degree of crystallinity
		a-Axis (Å)	c-Axis (Å)	Cell Vol. (Å) <sup>3</sup>	(% X <sub>c</sub> )
$\beta$ -TCP	$\text{Ca}_{8.88}(\text{PO}_4)_6$	10.4381	37.3943	3531.2669	85
1Zn- $\beta$ TCP	$\text{Ca}_{8.63} \text{Zn}_{0.25}(\text{PO}_4)_6$	10.4375	37.3645	3526.3572	75
2Zn- $\beta$ TCP	$\text{Ca}_{8.38} \text{Zn}_{0.5}(\text{PO}_4)_6$	10.4337	37.2474	3521.3914	79
3Zn- $\beta$ TCP	$\text{Ca}_{8.13} \text{Zn}_{0.75}(\text{PO}_4)_6$	10.4309	37.2217	3518.4521	64
4Zn- $\beta$ TCP	$\text{Ca}_{7.88} \text{Zn}_1(\text{PO}_4)_6$	10.4276	37.2035	3512.6672	59

O–P–O bonds, while the bands observed at 934, 1030, and 1124  $\text{cm}^{-1}$  were attributable to the stretching modes ( $\nu_3$  and  $\nu_1$ ) of P–O. In addition, the bands at 1640 and 3445  $\text{cm}^{-1}$  are a consequence of adsorbed water in the sample. The phosphate ( $\text{PO}_4^{3-}$ ) band widened and shifted from 965  $\text{cm}^{-1}$  to 940  $\text{cm}^{-1}$  and 1123  $\text{cm}^{-1}$  to 1157  $\text{cm}^{-1}$  in response to the doping of  $\text{Zn}^{2+}$  ion into  $\beta$ -TCP. This finding is likely a result of the lower level of crystallinity, as observed in the XRD analysis (Fig. 1) [26]. We can ascertain that the samples were hydroxyapatite-free, given the lack of peak formation at 630  $\text{cm}^{-1}$  and 3570  $\text{cm}^{-1}$  [6].

The morphology and structure at the level of the elements were investigated by field emission scanning electron microscopy (FESEM) in combination with Energy

Dispersive X-Ray (EDX). Fig. 3 presents the FESEM micrographs of the pure  $\beta$ -TCP powders and Zn- $\beta$ -TCP calcined at 1000 °C. Fig. 3(a) shows that the samples present as compact, irregular masses, with microporous surface structures (Fig. 3). Furthermore, the micrographs demonstrate a creation between particulates, a decrease in size, and an increase in  $\text{Zn}^{2+}$  content. Actual levels of  $\text{Zn}^{2+}$  doping, shown to have successfully obtained via EDX analysis, correlated with the calculated theoretical values (Table 3). Furthermore, the combined data from EDX and the changes to peak height, width, and shifting observed by XRD (Fig. 1) confirms that the substitution by  $\text{Zn}^{2+}$  ions occurred within the crystal structure and not only as surface absorption on  $\beta$ -TCP.

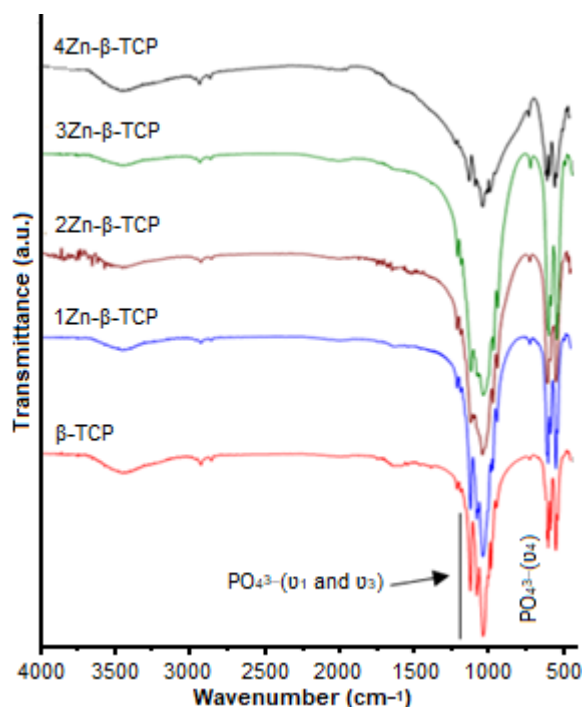


Fig 2. FTIR spectrum of  $\beta$ -TCP and Zn- $\beta$ -TCP

Table 3. Chemical composition of  $\beta$ -TCP and Zn- $\beta$ -TCP series by EDX

Samples	Theoretical ratios	Measured ratios
	Zn/Ca + Zn = $X_{Zn}$	Zn/Ca + Zn = $X_{Zn}$
$\beta$ -TCP	0.000	0.000
1Zn- $\beta$ -TCP	0.025	0.022
2Zn- $\beta$ -TCP	0.050	0.049
3Zn- $\beta$ -TCP	0.075	0.073
4Zn- $\beta$ -TCP	0.100	0.097

## CONCLUSION

Zinc is an essential trace element, which has been shown to promote bone formation both in vitro and in vivo, and  $\beta$ -TCP is an effective carrier of zinc. We successfully produced phases of Zn-doped  $\beta$ -TCP powders, using a microwave irradiation methodology. The integration of the zinc ions within the crystal structure was confirmed by EDX. The zinc ions decreased the crystallinity of the product as confirmed by XRD and FTIR spectroscopy. The overall cell volume decreased as a result of the substitution of the calcium ion by the smaller ionic radius of the zinc ion. The lattice parameter on a and c axes was also demonstrated to be smaller in the zinc-doped product. The changes in the morphology confirmed by FESEM showed a substantial change from densely packed nanoflakes to micron-sized microporous granules, which became smaller as zinc content in the doped  $\beta$ -TCP increased. We propose that the prepared powders will be widely useful and applicable to a range of biomedical applications.

## REFERENCES

- [1] Zhou, H., Agarwal, A.K., Goel, V.K., and Bhaduri, S.B., 2013, Microwave-assisted preparation of magnesium phosphate cement (MPC) for orthopedic applications: A novel solution to the exothermicity problem, *Mater. Sci. Eng., C*, 33 (7), 4288–4294.

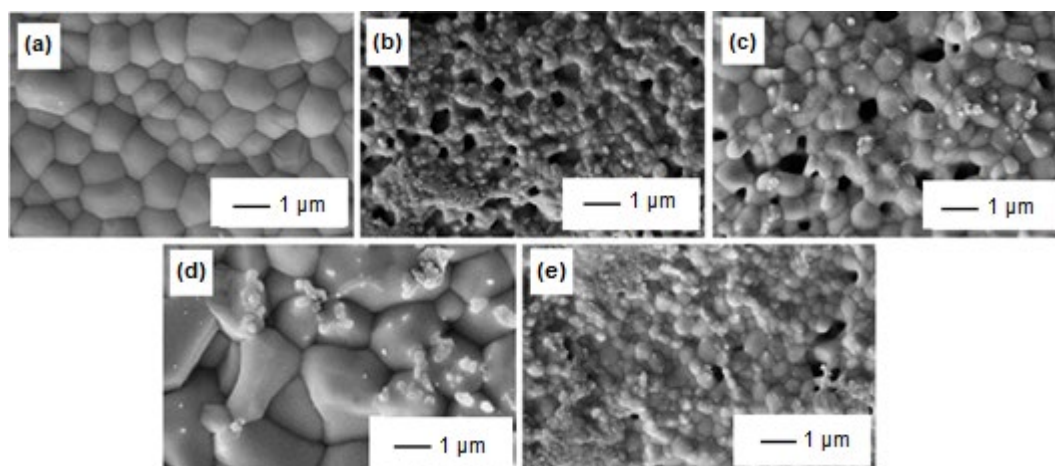


Fig 3. FESEM images showing the morphology of (a)  $\beta$ -TCP, (b) 1Zn- $\beta$ -TCP, (c) 2Zn- $\beta$ -TCP, (d) 3Zn- $\beta$ -TCP, and (e) 4Zn- $\beta$ -TCP calcination at 1000 °C

- [2] Taha, A., Akram, M., Jawad, Z., Alshemary, A.Z., and Hussain, R., 2017, Strontium doped injectable bone cement for potential drug delivery applications, *Mater. Sci. Eng., C*, 80, 93–101.
- [3] Gozalian, A., Behnamghader, A., Daliri, M., and Moshkforoush, A., 2011, Synthesis and thermal behavior of Mg-doped calcium phosphate nanopowders via the sol gel method, *Sci. Iran.*, 18 (6), 1614–1622.
- [4] Torres, P.M.C., Gouveia, S., Olhero, S., Kaushal, A., and Ferreira, J.M.F., 2015, Injectability of calcium phosphate pastes: Effects of particle size and state of aggregation of  $\beta$ -tricalcium phosphate powders, *Acta Biomater.*, 21, 204–216.
- [5] Zhang, J., Liu, W., Schnitzler, V., Tancret, F., and Bouler, J.M., 2014, Calcium phosphate cements for bone substitution: Chemistry, handling, and mechanical properties, *Acta Biomater.*, 10 (3), 1035–1049.
- [6] Saleh, A.T., Ling, L.S., and Hussain, R., 2016, Injectable magnesium-doped brushite cement for controlled drug release application, *J. Mater. Sci.*, 51 (16), 7427–7439.
- [7] Zhao, J., Zhao, J., Chen, J.H., Wang, X.H., Han, Z., and Li, Y., 2014, Rietveld refinement of hydroxyapatite, tricalcium phosphate and biphasic materials prepared by solution combustion method, *Ceram. Int.*, 40 (2) 3379–3388.
- [8] Xu, H.H.K., Carey, L.E., Simon, C.G., Takagi, S., and Chow, L.C., 2007, Premixed calcium phosphate cements: Synthesis, physical properties, and cell cytotoxicity, *Dent. Mater.*, 23 (4), 433–441.
- [9] Forouzandeh, A., Hesaraki, S., and Zamanian, A., 2014, The releasing behavior and in vitro osteoinductive evaluations of dexamethasone-loaded porous calcium phosphate cements, *Ceram. Int.*, 40 (1, Part A), 1081–1091.
- [10] Ribeiro, G.B.M., Trommer, R.M., dos Santos, L.A., and Bergmann, C.P., 2011, Novel method to produce  $\beta$ -TCP scaffolds, *Mater. Lett.*, 65 (2), 275–277.
- [11] Ma, H., Feng, C., Chang, J., and Wu, C., 2018, 3D-printed bioceramic scaffolds: From bone tissue engineering to tumor therapy, *Acta Biomater.*, 79, 37–59.
- [12] Han, B., Ma, P.W., Zhang, L.L., Yin, Y.J., Yao, K.D., Zhang, F.J., Zhang, Y.D., Li, X.L., and Nie, W., 2009,  $\beta$ -TCP/MCPM-based premixed calcium phosphate cements, *Acta Biomater.*, 5 (8), 3165–3177.
- [13] Pina, S., Torres, P.M.C., and Ferreira, J.M.F., 2010, Injectability of brushite-forming Mg-substituted and Sr-substituted  $\alpha$ -TCP bone cements, *J. Mater. Sci. - Mater. Med.*, 21 (2), 431–438.
- [14] Yashima, M., Sakai, A., Kamiyama, T., and Hoshikawa, A., 2003, Crystal structure analysis of  $\beta$ -tricalcium phosphate  $\text{Ca}_3(\text{PO}_4)_2$  by neutron powder diffraction, *J. Solid State Chem.*, 175 (2), 272–277.
- [15] Carrodegua, R.G., and De Aza, S., 2011,  $\alpha$ -Tricalcium phosphate: Synthesis, properties, and biomedical applications, *Acta Biomater.*, 7 (10), 3536–3546.
- [16] Cacciotti, I., and Bianco, A., 2011, High thermally stable Mg-substituted tricalcium phosphate via precipitation, *Ceram. Int.*, 37 (1), 127–137.
- [17] Kannan, S., Goetz-Neunhoeffler, F., Neubauer, J., Pina, S., Torres, P.M.C., and Ferreira, J.M.F., 2010, Synthesis and structural characterization of strontium- and magnesium-co-substituted  $\beta$ -tricalcium phosphate, *Acta Biomater.*, 6 (2), 571–576.
- [18] Tamimi, F., Sheikh, Z., and Barralet, J., 2012, Dicalcium phosphate cements: Brushite and monetite, *Acta Biomater.*, 8 (2), 474–487.
- [19] Razali, N.N., and Sopyan, I., 2018, Incorporation of poly(vinyl alcohol) for the improved properties of hydrothermal derived calcium phosphate cements, *Indones. J. Chem.*, 18 (2), 354–361.
- [20] Alshemary, A.Z., Goh, Y.F., Shakir, I., and Hussain, R., 2015, Synthesis, characterization and optical properties of chromium doped  $\beta$ -Tricalcium phosphate, *Ceram. Int.*, 41 (1, Part B), 1663–1669.
- [21] Zhang, S., Zhang, X., Cai, Q., Wang, B., Deng, X., and Yang, X., 2010, Microfibrous  $\beta$ -TCP/collagen scaffolds mimic woven bone in structure and composition, *Biomed. Mater.*, 5 (6), 065005.

- [22] Tao, J., Pan, H., Zhai, H., Wang, J., Li, L., Wu, J., Jiang, W., Xu, X., and Tang, R., 2009, Controls of tricalcium phosphate single-crystal formation from its amorphous precursor by interfacial energy, *Cryst. Growth Des.*, 9 (7), 3154–3160.
- [23] Shayegan, A., Petein, M., and Vanden Abbeele, A., 2009, The use of beta-tricalcium phosphate, white MTA, white Portland cement and calcium hydroxide for direct pulp capping of primary pig teeth, *Dent. Traumatol.*, 25 (4), 413–419.
- [24] Gbureck, U., Barralet, J.E., Spatz, K., Grover, L.M., and Thull, R., 2004, Ionic modification of calcium phosphate cement viscosity. Part I: Hypodermic injection and strength improvement of apatite cement, *Biomaterials*, 25 (11), 2187–2195.
- [25] Torres, P.M.C., Abrantes, J.C.C., Kaushal, A., Pina, S., Döbelin, N., Bohner, M., and Ferreira, J.M.F., 2016, Influence of Mg-doping, calcium pyrophosphate impurities and cooling rate on the allotropic  $\alpha \leftrightarrow \beta$ -tricalcium phosphate phase transformations, *J. Eur. Ceram. Soc.*, 36 (3), 817–827.
- [26] Dong, L., He, G., and Deng, C., 2016, Effects of strontium substitution on the phase transformation and crystal structure of calcium phosphate derived by chemical precipitation, *Ceram. Int.*, 42 (10), 11918–11923.